Aquaporin 7 deficiency is associated with development of obesity through activation of adipose glycerol kinase

Toshiyuki Hibuse*[†], Norikazu Maeda*[†], Tohru Funahashi*[‡], Kaori Yamamoto*, Azumi Nagasawa*, Wataru Mizunoya[§], Ken Kishida*, Kazuo Inoue[§], Hiroshi Kuriyama*, Tadashi Nakamura*, Tohru Fushiki[§], Shinji Kihara*, and Iichiro Shimomura*

*Department of Internal Medicine and Molecular Science, Graduate School of Medicine, Osaka University, 2-2-B5 Yamada-oka, Suita, Osaka 565-0871, Japan; and §Laboratory of Nutrition Chemistry, Division of Food Science and Biotechnology, Graduate School of Agriculture, Kyoto University, Kitashirakawa, Sakyo-ku, Kyoto 606-8502, Japan

In adipocytes, hydrolysis of triglycerides results in the release of free fatty acids and glycerol. Aquaporin 7 (AQP7), a member of aquaglyceroporins, is known to permeabilize glycerol and water. We recently generated *Aqp7*-knockout (KO) mice and demonstrated that such mice have low plasma glycerol levels and impaired glycerol release in response to β3-adrenergic agonist, suggesting that AQP7 acts as a glycerol gateway molecule in adipocytes for the efficient release of glycerol *in vivo*. Although there was no difference in body weight between WT and KO mice until 10 weeks of age, here we found that KO mice developed adult-onset obesity. The body weight and fat mass increased significantly in KO mice compared with WT mice after 12 weeks of age. Adipocytes of KO mice were large and exhibited accumulation of triglycerides compared with WT mice. The KO mice developed obesity and insulin resistance even at a young age after consumption of high-fat/high-sucrose diet. We demonstrated the enhanced glycerol kinase enzymatic activity in *Aqp7*-KO and -knockdown adipocytes. A series of our results indicate that AQP7 disruption elevates adipose glycerol kinase activity, accelerates triglycerides synthesis in adipocytes, and, finally, develops obesity.

adipocyte | insulin resistance | triglyceride | fatty acid

Aquaporins (AQPs) are a family of homologous water channels that are widely distributed in vertebrates, invertebrates, unicellular organism, and plants (1–3). A series of investigations showed that AQPs play a crucial role in water homeostasis (4, 5). AQP3, 7, 9, and 10 are subcategorized as aquaglyceroporins that permeabilize glycerol and water (6, 7). The AQP3 is expressed in epidermal cells and acts as a glycerol channel, which serves to maintain skin hydration, elasticity, and barrier function (8–10). Liver-specific aquaglyceroporin AQP9 is negatively regulated by insulin at a transcriptional level and thought to be an efficient gateway molecule incorporating glycerol as a substrate for gluconeogenesis in fasted state (11, 12).

We previously cloned a cDNA belonging to aquaglyceroporin from human adipose tissue cDNA library, designated AQP adipose (AQPap) (13). Subsequently, other groups showed that AQPap was a human homologue of AQP7, which was cloned from the rat testis (14). AQP7 is expressed abundantly in adipose tissues and is recognized as a sole glycerol channel of adipocyte at present (15). Adipose AQP7 is involved in glucose and glycerol metabolism based on marked modulation of its expression by dietary conditions (16). Recently, we generated the *Aqp7*-knockout (KO) mice and demonstrated that AQP7 serves as an adipose glycerol channel *in vivo*, and fat-derived glycerol determines fasting plasma glucose level (17). At present, the influence of AQP7 deficiency on adipocytes is not fully understood. The results of this study demonstrated that KO mice developed obesity after severe insulin resistance, and that the lack of AQP7 induced glycerol kinase activity and accumulation of triglycerides in adipocytes.

Materials and Methods

Animals and Physiological Experiments. *Aqp7* KO mice were generated as described in ref. 17. We analyzed mice backcrossed to C57BL/6N for five generations. Mice were fed with CRF-1 (Oriental Yeast, Suita, Japan) or high-fat/high sucrose (HF/HS) diet. The composition of the HF/HS diet was 14% beef tallow, 14% lard, 2% soybean oil, 20% sucrose, 25% milk casein, 15% corn starch, 5% cellulose, 3.5% mineral mixture, and 1% vitamin mixture (Oriental Yeast). Mice were kept at 22°C with a 12/12 h dark/light cycle (light cycle, 0800–2000 hours). Rectal temperature was measured by using a BAT-12 and microprobe RET-2 (Physitemp, Clifton, NJ) under the same condition (from 0900 to 1100 hours). Respiratory gas analysis was performed by using eight acrylic metabolic chambers, gas analyzers (model RL-600), and a switching system (model ANI6-A-S) as described in ref. 18. All experiments were conducted in male mice. The experimental protocol was approved by the Ethics Review Committee for Animal Experimentation of Osaka University School of Medicine.

Assessment of Metabolic Parameter and Regulation. Plasma glucose, insulin, and free fatty acid concentrations were measured by the Glucose CII-Test (Wako Pure Chemical, Osaka), the Insulin Measurement ELISA kit (Morinaga, Yokohama, Japan), and the Nescauto NEFA kit (Azwell, Osaka), respectively. Glycerol concentrations in plasma, medium, and tissues were determined by using a fluorometric/colormetric enzyme method. Plasma leptin and adiponectin levels were measured by the Leptin Measurement ELISA kit (Morinaga, Yokohama, Japan), and the Adiponectin ELISA kit (Otsuka, Tokushima, Japan), respectively. Tissue triglyceride and DNA contents were examined as described in ref. 19. Glucose and insulin tolerance tests were conducted as described in ref. 17.

Histological Analysis. An epididymal fat pad was excised from each mouse at 20 weeks of age. The isolated adipose tissues were formalin-fixed, paraffin-embedded, and subsequently cut into 6-μm sections and mounted on glass slides by using standard procedures. Finally, the adipose tissues were stained with hematoxylin and eosin. Adipocyte areas were measured in 200 or more cells per mouse by using MACSCOPE (Mitani, Fukui, Japan).

Fig. 1. Growth and metabolic parameters of KO mice under normal chow diet. (*A*) Growth curves of WT (*n* = 55) and KO (*n* = 62) mice. (*B*) Appearance of 20-week-old mice. (*C*) Metabolic parameters of 20-week-old mice under a 12-h fasting state (WT, *n* = 8; KO, *n* = 7). In *A* and *C*, data are mean ± SEM. *, *P* < 0.05; **, *P* < 0.01; compared with the values of WT mice under the same conditions.

Evaluation of Insulin Signaling. Twelve-hour-overnight-fasted mice were injected with either human regular insulin (1 unit/g of body weight) or saline through the inferior vena cava, and gastrocnemius muscle, epididymal fat, and liver were excised at 2, 3, and 4 min after injection, respectively. Tissue samples were homogenized and centrifuged at $15,000 \times g$ for 30 min in ice-cold homogenization buffer described in ref. 20. The supernatants were collected, and protein concentration was measured with BCA Protein Assay Kit (Pierce) by using BSA as a standard. A 30-μg protein sample was boiled for 5 min, cooled on ice, and subjected to 12.5% SDS/PAGE, followed by transblotting to a nitrocellulose membrane. Western blot analysis was carried out by using antibodies to Akt and Phospho-Akt (Cell Signaling Technology, Beverly, MA). Insulin receptor substrate (IRS)-associated phosphatidylinositol 3-kinase (PI3-kinase) activity assay was conducted as described in ref. 20. Briefly, equal amounts of extracted protein were immunoprecipitated with anti-IRS-1 or anti-IRS-2 antibodies (Upstate Biotechnology, Lake Placid, NY), followed by rinsing with PI3-kinase buffer [25 mM Tris·HCl, pH 7.4/0.5 mM EGTA/100 mM NaCl]. The reaction was initiated by adding 55 μl of reaction buffer [10 μg of L-α-phosphatidylinositol/200 μM ATP/200 mM MgCl$_2$/25 mM Tris·HCl, pH 7.4/0.5 mM EGTA/100 mM NaCl/10 μCi [γ-^{32}P]ATP (1 Ci = 37 GBq)] and then incubated for 20 min at room temperature. The reaction was terminated by 180 μl of stop solution (CHCl$_3$:methanol:11.6 M HCl = 100:100:1), and the organic phase was separated by centrifugation and washed with methanol, 1M HCl (1:1). The lipids were spotted onto Silica Gel 60 Plate (Merck) and developed in a mixture of CHCl$_3$:methanol:28% ammonium hydroxide:water (43:38:5:7). The phosphorylated lipids were visualized by autoradiography, and the radioactive spots were quantified by FAST SCAN Scanning Imager (Molecular Dynamics).

Cell Culture and Transfection of RNA Interference (RNAi). The mouse 3T3-L1 cell line was obtained from Health Science Research Resources Bank (Osaka). 3T3-L1 preadipocytes were grown to confluence and induced to differentiate into adipocytes as described in ref. 15. The sequences of the sense RNAi were previously noted in ref. 17. Control or *Aqp7* RNAi was transfected into 3T3-L1 adipocytes by using Lipofectamine 2000 (Invitrogen). Twenty-four hours after transfection, the cells were subjected to glycerol kinase activity assay and oleic acid uptake assay, as described below.

Determination of Mouse Glycerol Kinase (Gyk) Activity. Gyk activity assay was performed as described previously in ref. 21. Briefly, white adipose tissues or differentiated 3T3-L1 adipocytes were homogenized in extraction buffer (50 mM Hepes, pH 7.8/40 mM KCl/11 mM MgCl$_2$/1 mM EDTA/1 mM DTT) on ice, and centrifuged at $15,000 \times g$ for 15 min at 4°C. Ten-microgram protein was used for enzymatic assay. The protein samples were incubated with 50 μl of assay buffer (50 mM Tris·HCl, pH 7.2/5 mM ATP/10 mM MgCl$_2$/100 mM KCl/2.5 mM DTT/4 mM glycerol/500 μM ^{3}H-glycerol) for 90 min at 37°C. The reaction was terminated with 100 μl of stop solution (ethanol:methanol, 97:3). Equal amounts of the sample (20 μl) were spotted onto DE81 Whatman filters (Whatman), and then the filters were air dried and washed in water overnight. Radioactivity adhering to the filters was measured by liquid scintillation.

Oleic Acid Uptake. Oleic acid uptake assay was performed as described in refs. 21 and 22. After serum deprivation, 3T3-L1 adipocytes cultured in 12-well plates were incubated for 3 h in Kreb's–Ringer Hepes buffer (128 mM NaCl/5.2 mM KCl/1.4 mM MgSO$_4$/1.4 mM CaCl$_2$/5 mM KH$_2$PO$_4$/10 mM Hepes, pH 7.4) with 1 μM epinephrine. The assay was initiated by the addition of 50 μM oleic acid containing [9, 10(n)-^{3}H]oleic acid (5 μCi per well), 50 μM D(+)-glucose, and 100 μM fatty acid-free BSA. After 90 min, uptake was terminated by 200 μM phloretin, and cells were vigorously washed three times in ice-cold PBS. The cells were collected and homogenized in 0.5 M NaOH, and an aliquot was used to determine radioactivity by liquid scintillation counting.

Statistical Analysis. Results were expressed as the mean ± SEM of *n* separate experiments. Differences between groups were examined for statistical significance by using Student's *t* test or ANOVA with Fisher's protected least significant difference test.

Results

We analyzed the growth of WT and KO mice under the normal chow diet from 6 to 24 weeks of age. KO mice had similar body weight compared with WT mice until 10 weeks of age, as reported in our previous study (17). However, the body weight increased significantly in KO mice compared with WT mice after 12 weeks of age (Fig. 1*A*). This difference was not due to differences in food intake; there was no significant difference in food intake corrected to body weight between WT and KO mice at each week of age (data
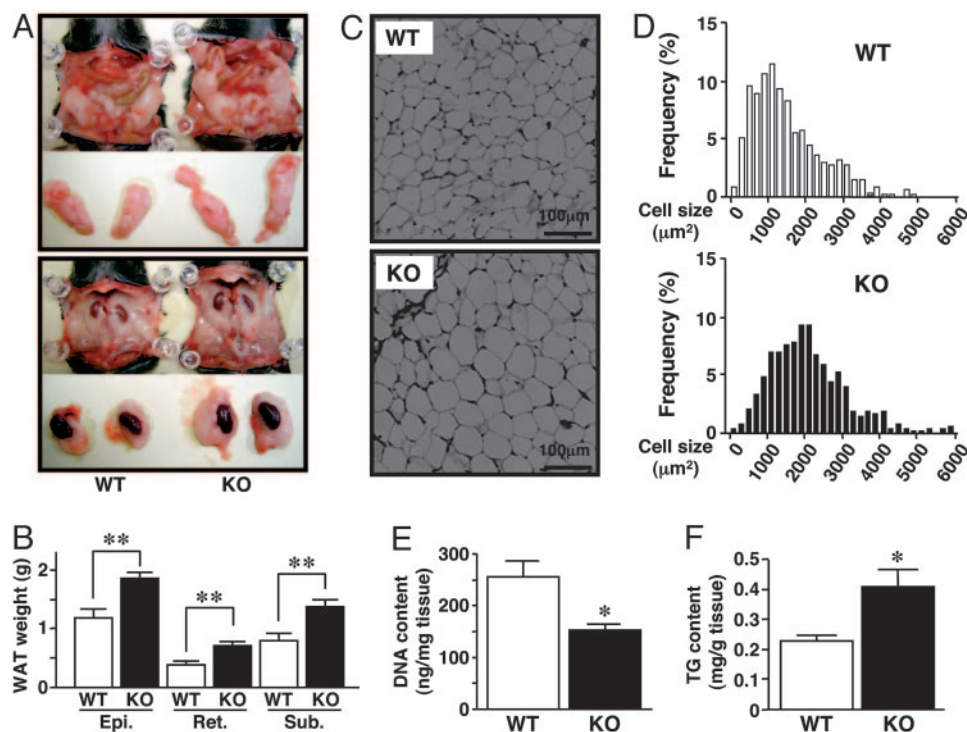
Fig. 2. Adipocyte hypertrophy in KO mice. Adipose tissues were excised from WT and KO mice at 20 weeks of age. (*A*) Appearance of epididymal (*Upper*) and retroperitoneal (*Lower*) fat. The top images show the ventral view of WT and KO mice. The bottom images indicate fat pads with testis and kidney, respectively. (*B*) Weights of various adipose tissues (*n* = 6 per group). (*C*) Histology of epididymal WAT. WAT sections were stained by hematoxylin and eosin after formalin fixation. (*D*) Cell size distribution of adipocytes in WT (*Upper*) and KO (*Lower*) mice. The area of white adipocyte was measured in 200 or more cells per mouse in the respective groups. (*E*) DNA content in WAT (*n* = 6 per group). (*F*) Triglyceride content in WAT (*n* = 6 per group). Epi, epididymal WAT; Ret, retroperitoneal WAT; Sub, s.c. WAT; TG, triglyceride. In *B*, *E*, and *F*, data are mean ± SEM. *, $P < 0.05$; **, $P < 0.01$; compared with the values of WT mice.

not shown). The photos shown in Fig. 1*B* were taken for representative mice of each group at 20 weeks of age. We measured metabolic parameters of these mice under a 12-h fasting state at 20 weeks of age (Fig. 1*C*). Plasma glucose, insulin, and free fatty acid concentrations were significantly higher in KO mice than in WT mice, but KO mice had significantly lower plasma glycerol levels under 12-h fasting conditions. Plasma concentrations of leptin, which is considered as an adiposity marker protein, were significantly higher in KO mice than in WT mice. Plasma concentrations of adiponectin, an insulin-sensitizing hormone derived from adipocytes, were significantly lower in KO mice than WT mice.

We excised various tissues from these mice and measured tissue weights. There were no marked differences in the weights of liver, kidney, gastrocnemius muscle, and heart between WT and KO mice (data not shown), but the fat pads of KO mice were significantly larger than those of WT mice (Fig. 2*A*). Epididymal, retroperitoneal, and s.c. white adipose tissues (WAT) of KO mice were significantly heavier than those of WT mice (Fig. 2*B*). Histological analysis of WAT showed that the size of lipid droplets was generally larger in KO mice than in WT mice (Fig. 2*C*). The cell size distribution of WAT demonstrated a marked increase of hypertrophic adipocytes in KO mice than in WT mice (Fig. 2*D*). DNA content in WAT was significantly decreased in KO mice (Fig. 2*E*). In contrast to DNA content, the triglyceride content in these tissues was higher in KO mice (Fig. 2*F*). These results indicated a larger size of adipocytes in KO mice than in WT mice.

Next, we examined insulin sensitivity in the 20-week-old mice. Insulin tolerance tests showed that insulin-mediated suppression of plasma glucose was disturbed in KO mice (Fig. 3*A*). Glucose tolerance tests also demonstrated severely impaired glucose tolerance in KO mice (Fig. 3*B*). We also evaluated insulin signaling in WAT, liver, and muscle. Insulin stimulation of IRS-1-associated PI3-kinase activity was markedly lower in WAT and muscle of KO mice than WT mice (Fig. 3*C*). IRS-2-associated PI3-kinase activities in the liver and muscle were also significantly lower in KO mice than in WT mice (Fig. 3*D*). Insulin-stimulated phosphorylation of Akt in WAT, liver, and muscle was significantly lower in KO mice

than in WT mice (Fig. 3*E*). These results suggested whole-body insulin resistance associated with adult-onset obesity in KO mice.

In other experiments, WT and KO mice were fed with HF/HS diet from 8 weeks of age, when both groups had similar body weight. The experimental protocol is shown schematically in Fig. 4*A*. Surprisingly, the body weight of KO mice increased rapidly and became significantly heavier than that of WT mice after 14 days of feeding with HF/HS diet (Fig. 4*B*). Furthermore, plasma glucose concentrations tended to be higher in KO mice, albeit insignificantly (Fig. 4*C*). Plasma insulin concentrations of KO mice were significantly higher than WT mice after day 7 on HF/HS diet (Fig. 4*D*). We further examined insulin and glucose tolerance tests after 4 weeks of HF/HS diet (12 weeks of age). Insulin tolerance test demonstrated that insulin-mediated suppression of plasma glucose was severely impaired in KO mice than in WT mice (Fig. 4*E*). Glucose tolerance test showed that plasma glucose concentrations were slightly higher in KO mice than in WT mice (Fig. 4*F*). The results of HF/HS diet study suggested that KO mice were vulnerable to diet-induced obesity and insulin resistance.

Why was AQP7 deficiency associated with the development of obesity? To elucidate the underlying mechanism, we analyzed these mice at 6–10 weeks of age, when there was no difference in body weight between WT and KO mice. Examination of O_2 consumption at 10 weeks of age showed no significant difference in O_2 consumption between WT and KO mice (Fig. 5*A*). Furthermore, there was no significant difference in rectal temperature between WT and KO mice before 19 weeks of age (Fig. 5*B*). However, rectal temperature of KO mice became significantly lower than WT mice after 20 weeks of age, when obesity developed in KO mice. These results suggested that the metabolic rate of WT and KO mice was almost similar at identical body weight. In the same 10-week-old mice, we examined the mRNA levels of uncoupling protein (*Ucp*), *Cd36*, solute carrier family 27 (fatty acid transporter) member 1 (*Slc27a1*), lipoprotein lipase (*Lpl*), insulin receptor substrates (*Irs*), diacylglycerol *O*-acyltransferase (*Dgat*), perilipin (*Plin*), lipase, hormone sensitive (*Lipe*), adiponectin, C1Q- and collagen-domain containing (*Adipoq*), leptin (*Lep*), fatty acid binding protein 4, adipocyte (*Fabp4*), peroxisome proliferator-activated receptor γ
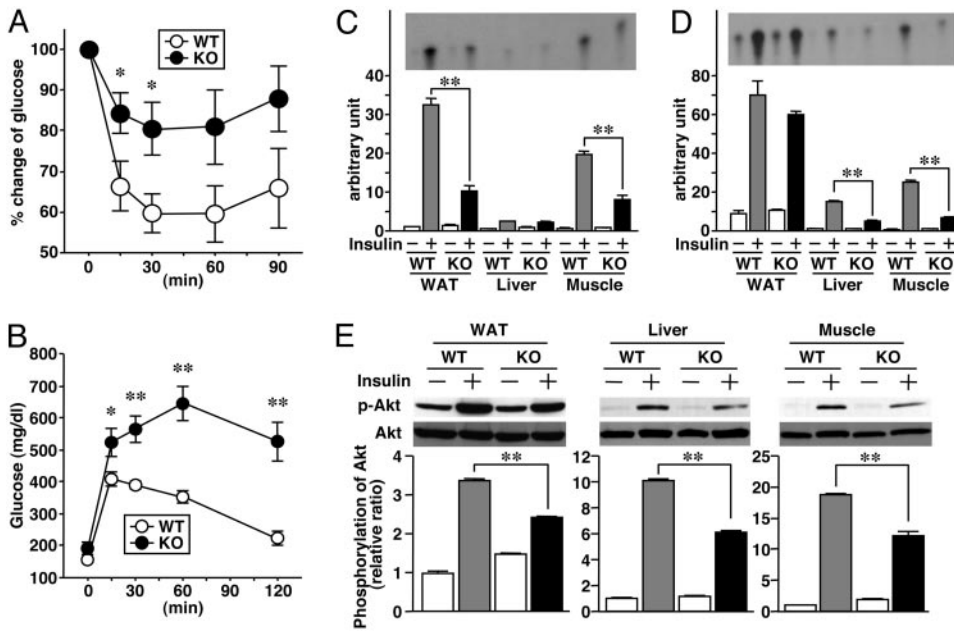
Fig. 3. Whole-body insulin resistance associated with obesity in KO mice. Mice were examined at 20 weeks of age. (*A*) Glucose curves under insulin tolerance test (*n* = 8 per group). Plasma glucose concentrations were normalized to those at 0 min (100%). (*B*) Glucose curves from a glucose tolerance test (*n* = 8 per group). (*C* and *D*) Insulin-stimulated IRS-1-associated (*C*) and IRS-2-associated (*D*) PI3-kinase activity (*n* = 5 per group). ^{32}P-labeled 3-phosphatidylinositides were quantified as described in *Materials and Methods*. (*E*) Insulin-stimulated phosphorylation of Akt (*n* = 5 per group). Equal amounts of protein were immunoblotted with anti-phospho-Akt and anti-Akt antibodies. Phosphorylated-Akt and Akt signal was quantified by a scanning imager. The relative ratio of Akt phosphorylation was calculated after normalization with Akt signal and normalized in WT mice without insulin in respective tissues. WAT, epididymal white adipose tissue. Data are mean ± SEM. *, $P < 0.05$; **, $P < 0.01$; compared with WT mice under same condition.

(*Pparg*), CCAAT/enhancer binding protein (C/EBP) α (*Cebpa*) in WAT and brown adipose tissue (BAT), which are related to thermogenesis, fatty acids uptake, insulin signal, lipogenesis, lipolysis, and adipogenesis (23). There were no apparent changes in these mRNA levels between WT and KO mice under both fed (data not shown) and 12-h fasted state (Fig. 5*C*), when the body weight of KO mice was similar to that of WT mice. Our recent study in *Aqp7* null mice showed that WAT glycerol contents were significantly elevated in KO mice (17). We postulated that glycerol might be reincorporated into triglycerides in the AQP7-deficient adipocytes. We first measured mRNA levels and activities of adipose Gyk, which is a key enzyme that converts glycerol to glycerol-3-phosphate (glycerol-3-P), in these mice at 10 weeks of age. No significant difference was detected in Gyk mRNA levels in adipose tissues of WT and KO mice (data not shown). However, adipose Gyk enzymatic activity of KO mice was significantly higher than

that of WT mice under the 12-h fasting state (Fig. 6*A*). To confirm the effect of AQP7 deficiency on adipocytes, we knocked down *Aqp7* in 3T3-L1 adipocytes by using RNAi. Knockdown of *Aqp7* in adipocytes was associated with a significant reduction of glycerol in the media (Fig. 6*B*) and a significant increase in glycerol content in cell lysate (Fig. 6*C*). There was no difference in Gyk mRNA level between control- and *Aqp7*-RNAi transfected adipocytes (data not shown), whereas a 4-fold enzymatic activation of Gyk was observed in *Aqp7*-knockdown adipocytes (Fig. 6*D*). In a series of *in vitro* experiments, we performed an oleic acid uptake assay. The uptake of oleic acid significantly increased in *Aqp7*-knockdown 3T3-L1 adipocytes (Fig. 6*E*). Finally, triglyceride content was significantly elevated in *Aqp7*-knockdown adipocytes (Fig. 6*F*).

Discussion

The major finding of this study was that deficiency of the adipose glycerol channel AQP7 was associated with obesity. On the cellular
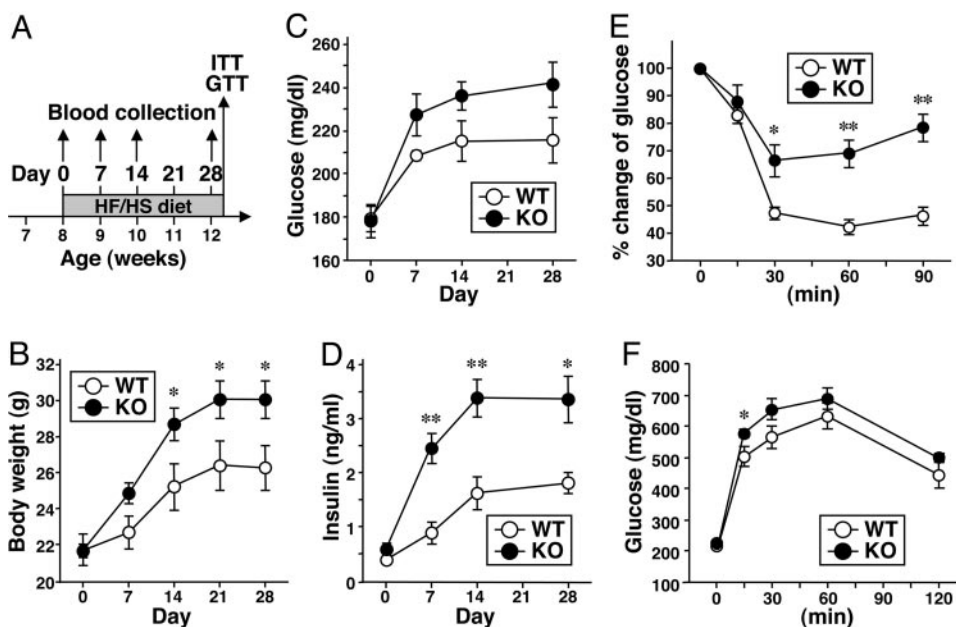

Fig. 4. Diet-induced obesity in KO mice. (*A*) The protocol of HF/HS diet study. Mice were started on HF/HS diet at 8 weeks of age, when there were no differences in body weight between WT (*n* = 5) and KO (*n* = 8) mice. (*B–D*) Shown is the effect of HF/HS diet on body weight (*B*), plasma glucose (*C*), and plasma insulin (*D*). (*E*) Glucose curves under the insulin tolerance test after 4 weeks HF/HS diet. Plasma glucose concentrations were normalized to those at 0 min (100%). (*F*) Glucose curves from the glucose tolerance test. In *B*, *D*, *E*, and *F*, data are mean ± SEM. *, $P < 0.05$; **, $P < 0.01$; compared with the values of WT mice under the same conditions.
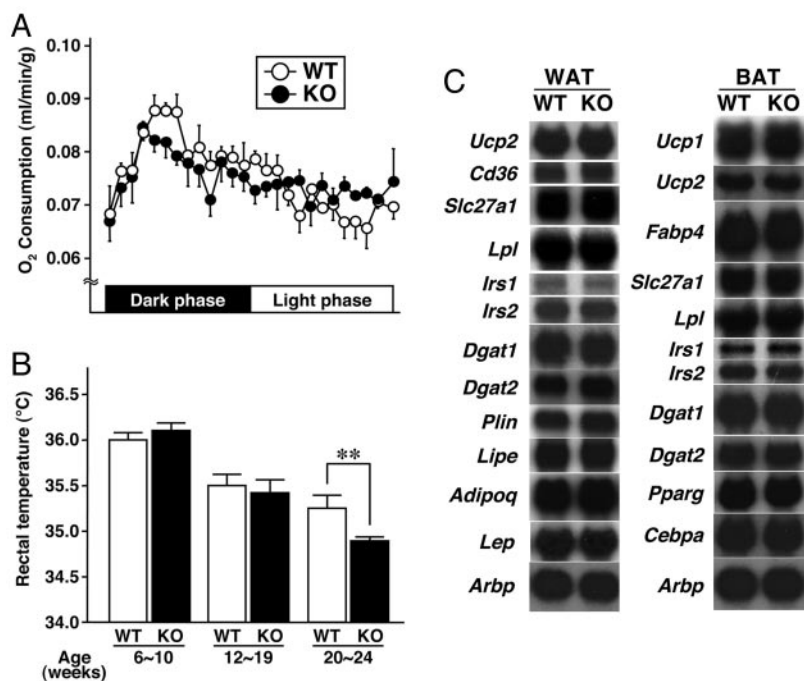
Fig. 5. Physiological and molecular analysis of metabolic function. (*A*) O₂ consumption in WT and KO mice at 10 weeks of age (*n* = 4 per group). (*B*) Rectal temperature at 6–10 weeks of age (WT, *n* = 90; KO, *n* = 57), 12–19 weeks of age (WT, *n* = 29; KO, *n* = 29), and 20–24 weeks of age (WT, *n* = 19; KO, *n* = 25). (*C*) Northern blot analysis of mRNAs of *Ucp*, uncoupling protein; *Cd36*, CD36 antigen; *Slc27a1*, solute carrier family 27 (fatty acid transporter), member 1; *Lpl*, lipoprotein lipase; *Irs*, insulin receptor substrate; *Dgat*, diacylglycerol O-acyltransferase; *Plin*, perilipin; *Lipe*, lipase, hormone sensitive; *Adipoq*, adiponectin, C1Q, and collagen domain containing; *Lep*, leptin; *Fabp4*, fatty acid binding protein 4, adipocyte; *Pparg*, peroxisome proliferator-activated receptor γ; *Cebpa*, CCAAT/enhancer binding protein (C/EBP) α; *Arbp*, acidic ribosomal phosphoprotein P0 (36B4) in WAT (white adipose tissue) and BAT (brown adipose tissue). In *A* and *B*, data are mean ± SEM. ∗∗, *P* < 0.01 compared with WT mice.

level, disruption of adipose AQP7 increased intracellular glycerol content, enhanced adipose Gyk enzymatic activity, and resulted in accumulation of triglycerides in adipocytes (Fig. 6*G*). There were no significant differences in mRNA levels of various molecules in

adipose tissue related to lipolysis, lipogenesis, and thermogenesis between WT and KO mice at 10 weeks of age. We confirmed that the above changes were not due to differences in O₂ consumption or core temperature before the development of obesity in KO mice.
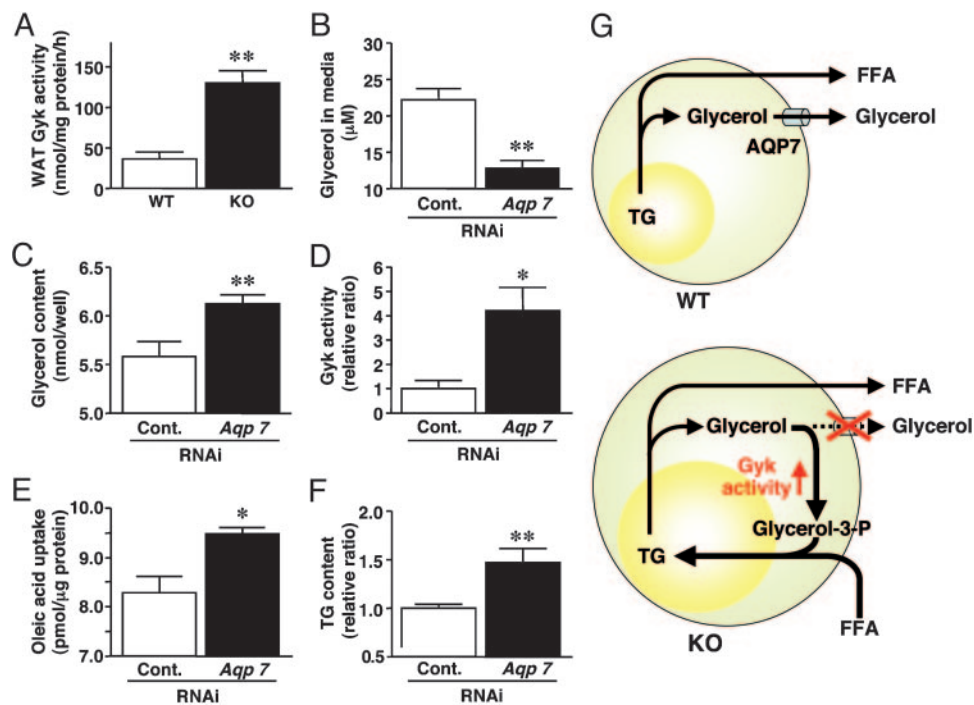
Fig. 6. Enhanced adipose glycerol kinase enzymatic activity in *Aqp7*-KO and -knockdown adipocytes. (*A*) Gyk enzymatic activity in WAT of WT and KO mice under 12-h fasting condition (*n* = 6 per group). (*B* and *C*) Glycerol concentrations in media (*B*) and glycerol contents in cell lysates (*C*) of *Aqp7*-knockdown 3T3-L1 adipocytes (*n* = 6 per group). (*D*) Gyk enzymatic activity in 3T3-L1 adipocytes transfected with RNAi. Shown are folds of induction calculated based on the activity from transfections with control RNAi (*n* = 6 per group). (*E*) Uptake of oleic acid in 3T3-L1 adipocytes transfected with RNAi (*n* = 6 per group). (*F*) Intracellular triglyceride (TG) contents in RNAi-transfected 3T3-L1 adipocytes (*n* = 6 per group). (*G*) Schematic presentation of the mechanism of obesity in *Aqp7* KO mice. AQP7 ensures efficient glycerol release from adipocytes in WT mice (*Upper*). Adipose AQP7 deficiency is associated with an increase of intracellular glycerol content. The latter enhances Gyk enzymatic activity converting glycerol to glycerol-3-P, promotes uptake of fatty acids, and finally results in TG accumulation in AQP7-deficient adipocytes (*Lower*). FFA, free fatty acid. In *A–F*, data are mean ± SEM. ∗, *P* < 0.05; ∗∗, *P* < 0.01; compared with WT mice or control RNAi.

Glycerol kinase (ATP:glycerol-3-phosphotransferase) is encoded in X chromosome and glycerol kinase deficiency in humans occurs as an isolated enzyme deficiency or as part of a contiguous gene deletion syndrome in variable association with Duchenne muscular dystrophy and/or congenital adrenal hypoplasia. Isolated glycerol kinase deficiency has an inconstant phenotype, ranging from asymptomatic hyperglycerolemia to a severe metabolic disorder with growth and psychomotor retardation (24–27). Gyk is a key enzyme that catalyzes the phosphorylation of glycerol to glycerol-3-P. Especially in fasted liver, Gyk enhances the conversion of incorporated glycerol to glycerol-3-P for gluconeogenesis in parallel with the up-regulation of phosphoenolpyruvate carboxykinase. Recently, Deutscher and coworkers (28) analyzed the crystal structure of Gyk in Gram-positive *Enterococcus casseliflavus* and determined the phosphorylation site, which resulted in 10- to 15-fold increase of Gyk enzymatic activity. They also demonstrated the catalytic cleft of Gyk, in which glycerol and ATP bind. Their results indicate that Gyk enzymatic activity is induced by glycerol itself. In this study, we found a significant decrease of liver Gyk enzymatic activity in 12-h fasting KO mice at 10 weeks of age (WT, 369.24 ± 12.43; KO, 267.54 ± 19.97 nmol·h^{-1} per mg of protein, $n = 5$–6, $P < 0.01$) in association with significant reduction of plasma glycerol in KO mice than WT mice. However, the role of adipose Gyk has not been elucidated, because Gyk expression level in WAT is lower than in other tissues. Lazar and coworkers demonstrated that thiazolidinedions markedly increased Gyk mRNA level in adipocytes, resulting in triglyceride accumulation through enhancement of the conversion of glycerol into glycerol-3-P (21). They showed that oleic acid uptake and triglyceride synthesis were significantly increased in adipocytes transfected with adenovirus expressing Gyk. Our results are in agreement with those of the above studies. Our data showed that intracellular accumulation of glycerol in *Aqp7*-KO and -knockdown adipocytes increased Gyk enzymatic activity, resulting in enhancement of fatty acid uptake and triglyceride accumulation. Further studies are necessary to investigate the role of Gyk in adipocytes by using adipose-specific Gyk-transgenic and/or -KO mice.

We previously reported a case of loss of function mutation in the AQP7 gene (Gly-264 to Val) (29). The increase of plasma glycerol in response to exercise was impaired in the subject with homozygous G264V mutation, but the subject was not obese or diabetic. We could not conclude that the functional AQP7 mutation in human is associated with obesity or diabetes, because our identified subject with homozygous G264V mutation was only a single case. Further analysis of human AQP7 gene and/or frequency of AQP7 mutation in obese subjects should be performed in the future.

Recently, Verkman and coworkers (30) reported the presence of large adipoctyes in *Aqp7* KO mice. They showed that the length of KO mice was reduced compared with WT mice, but the body weight of KO mice was similar to WT mice at 16 weeks of age. We also measured the length from nose to anus of WT and KO mice at several ages; however, there was no difference in length of these mice (WT, 9.11 ± 0.17 cm; KO, 9.01 ± 0.05 cm at 8 weeks of age, $n = 10$; WT, 9.95 ± 0.05 cm; KO, 9.90 ± 0.06 cm at 14 weeks of age, $n = 13$; and WT, 10.42 ± 0.05 cm; KO, 10.40 ± 0.05 cm at 20 weeks of age, $n = 8$). They analyzed *Aqp7* null mice backcrossed into CD1 genetic background, whereas we crossed *Aqp7* KO mice into C57BL/6N mice. We speculate that the different phenotypes of our KO mice and their KO mice depend on the genetic background. Our previous and present data agree with their data with regard to the similarity of lipolytic activity and impairment of glycerol permeability in WAT of WT and KO mice. Furthermore, our current study clearly demonstrated that AQP7 deficiency increases adipose Gyk enzymatic activity *in vivo* and *in vitro*, causing obesity and insulin resistance.

In summary, *Aqp7* KO mice exhibited adult-onset and diet-induced obesity associated with severe insulin resistance. Disruption of adipose AQP7 is associated with elevated glycerol kinase enzymatic activity through increased intracellular glycerol, increased uptake of fatty acid, and acceleration of triglycerides synthesis.

1. Denker, B. M., Smith, B. L., Kuhajda, F. P. & Agre, P. (1988) *J. Biol. Chem.* **263,** 15634–15642.
2. Verkman, A. S. (2002) *J. Anat.* **200,** 617–627.
3. Agre, P. & Kozono, D. (2003) *FEBS Lett.* **555,** 72–78.
4. Preston, G. M., Carroll, T. P., Guggino, W. B. & Agre, P. (1992) *Science* **256,** 385–387.
5. Giles, J. (2003) *Nature* **425,** 651.
6. Ishibashi, K., Sasaki, S., Fushimi, K., Uchida, S., Kuwahara, M., Saito, H., Furukawa, T., Nakajima, K., Yamaguchi, Y., Gojobori, T. & Marumo, F. (1994) *Proc. Natl. Acad. Sci. USA* **91,** 6269–6273.
7. Agre, P., King, L. S., Yasui, M., Guggino, W. B., Ottersen, O. P., Fujiyoshi, Y., Engel, A. & Nielsen, S. (2002) *J. Physiol. (London)* **542,** 3–16.
8. Ma, T., Hara, M., Sougrat, R., Verbavatz, J. M. & Verkman, A. S. (2002) *J. Biol. Chem.* **277,** 17147–17153.
9. Hara, M., Ma, T. & Verkman, A. S. (2002) *J. Biol. Chem.* **277,** 46616–46621.
10. Hara, M. & Verkman, A. S. (2003) *Proc. Natl. Acad. Sci. USA* **100,** 7360–7365.
11. Kuriyama, H., Shimomura, I., Kishida, K., Kondo, H., Furuyama, N., Nishizawa, H., Maeda, N., Matsuda, M., Nagaretani, H., Kihara, S., *et al.* (2002) *Diabetes* **51,** 2915–2921.
12. Carbrey, J. M., Gorelick-Feldman, D. A., Kozono, D., Praetorius, J., Nielsen, S. & Agre, P. (2003) *Proc. Natl. Acad. Sci. USA* **100,** 2945–2950.
13. Kuriyama, H., Kawamoto, S., Ishida, N., Ohno, I., Mita, S., Matsuzawa, Y. & Okubo, K. (1997) *Biochem. Biophys. Res. Commun.* **241,** 53–58.
14. Ishibashi, K., Kuwahara, M., Gu, Y., Kageyama, Y., Tohsaka, A., Suzuki, F., Marumo, F. & Sasaki, S. (1997) *J. Biol. Chem.* **272,** 20782–20786.
15. Kishida, K., Kuriyama, H., Funahashi, T., Shimomura, I., Kihara, S., Ouchi, N., Nishida, M., Nishizawa, H., Matsuda, M., Takahashi, M, *et al.* (2000) *J. Biol. Chem.* **275,** 20896–20902.
16. Kishida, K., Shimomura, I., Kondo, H., Kuriyama, H., Makino, Y., Nishizawa, H., Maeda, N., Matsuda, M., Ouchi, N., Kihara, S., *et al.* (2001) *J. Biol. Chem.* **276,** 36251–36260.
17. Maeda, N., Funahashi, T., Hibuse, T., Nagasawa, A., Kishida, K., Kuriyama, H., Nakamura, T., Kihara, S., Shimomura, I. & Matsuzawa, Y. (2004) *Proc. Natl. Acad. Sci. USA* **101,** 17801–17806.
18. Miyawaki, K., Yamada, Y., Ban, N., Ihara, Y., Tsukiyama, K., Zhou, H., Fujimoto, S., Oku, A., Tsuda, K, Toyokuni, S., *et al.* (2002) *Nat. Med.* **8,** 738–742.
19. Okuno, A., Tamemoto, H., Tobe, K., Ueki, K., Mori, Y., Iwamoto, K., Umesono, K., Akanuma, Y., Fujiwara, T., Horikoshi, H., *et al.* (1998) *J. Clin. Invest.* **101,** 1354–1361.
20. Maeda, N., Shimomura, I., Kishida, K., Nishizawa, H., Matsuda, M., Nagaretani, H., Furuyama, N., Kondo, H., Takahashi, M, Arita, Y., *et al.* (2002) *Nat. Med.* **8,** 731–737.
21. Guan, H. P., Li, Y., Jensen, M. V., Newgard, C. B., Steppan, C. M. & Lazar, M. A. (2002) *Nat. Med.* **8,** 1122–1128.
22. Ruan, H. & Pownall, H. J. (2001) *Diabetes* **50,** 233–240.
23. Spiegelman, B. M. & Flier, J. S. (2001) *Cell* **104,** 531–543.
24. Lin, E. C. (1977) *Annu. Rev. Biochem.* **46,** 765–795.
25. McCabe, E. R. B. (1995) *The Metabolic and Molecular Bases of Inherited Disease* (McGraw–Hill, New York), 7th Ed., 1631–1652.
26. Huq, A. H., Lovell, R. S., Ou, C. N., Beaudet, A. L. & Craigen, W. J. (1997) *Hum. Mol. Genet.* **6,** 1803–1809.
27. Dipple, K. M., Zhang, Y. H., Huang, B. L., McCabe, L. L., Dallongerille, J., Inokuchi, T., Kimura, M., Marx, H. J., Roederer, G. O., Shih, V., *et al.* (2001) *Hum. Genet.* **109,** 55–62.
28. Yeh, J. I., Charrier, V., Paulo, J., Hou, L., Darbon, E., Claiborne, A., Hol, W. G. & Deutscher, J. (2004) *Biochemistry* **43,** 362–373.
29. Kondo, H., Shimomura, I., Kishida, K., Kuriyama, H., Makino, Y., Nishizawa, H., Matsuda, M., Maeda, N., Nagaretani, H., Kihara, S., *et al.* (2002) *Eur. J. Biochem.* **269,** 1814–1826.
30. Hara-Chikuma, M., Sohara, E., Rai, T., Ikawa, M., Okabe, M., Sasaki, S., Uchida, S. & Verkman, A. S. (2005) *J. Biol. Chem.* **280,** 15493–15496.